

A Fermi Energy-Incorporated Framework for Dealing with the Temperature- and Magnetic Field-Dependent Critical Current Densities of Superconductors and Its Application to Bi-2212

Gulshan Prakash Malik¹, Vijaya Shankar Varma²

¹B-208, Sushant Lok 1, Gurgaon, Haryana, India

²180 Mall Apartments, Delhi, India

Email: gulshanpmalik@yahoo.com, varma2@gmail.com

How to cite this paper: Malik, G.P. and Varma, V.S. (2020) A Fermi Energy-Incorporated Framework for Dealing with the Temperature- and Magnetic Field-Dependent Critical Current Densities of Superconductors and Its Application to Bi-2212. *World Journal of Condensed Matter Physics*, **10**, 53-70.

<https://doi.org/10.4236/wjcmp.2020.102004>

Received: February 6, 2020

Accepted: March 15, 2020

Published: March 18, 2020

Copyright © 2020 by author(s) and Scientific Research Publishing Inc. This work is licensed under the Creative Commons Attribution International License (CC BY 4.0).

<http://creativecommons.org/licenses/by/4.0/>



Open Access

Abstract

It is well known that the critical current density of a superconductor depends on its size, shape, nature of doping and the manner of preparation. It is suggested here that the *collective* effect of such differences for different samples of the same superconductor is to endow them with different values of the Fermi energy—a single property to which may be attributed the observed variation in their critical current densities. The study reported here extends our earlier work concerned with the generalized BCS equations [Malik, G.P. (2010) *Physica B*, **405**, 3475-3481; Malik, G.P. (2013) *WJCM*, **3**, 103-110]. We develop here for the first time a framework of *microscopic* equations that incorporates all of the following parameters of a superconductor: temperature, momentum of Cooper pairs, Fermi energy, applied magnetic field and critical current density. As an application of this framework, we address the different values of critical current densities of Bi-2212 for non-zero values of temperature and applied magnetic field that have been reported in the literature.

Keywords

Generalized BCS Equations, Fermi Energy, Critical Current Density, Non-Zero Temperatures and Applied Fields, Bi-2212

1. Introduction

The critical current density (j_c) of a superconductor (SC) is an important parameter because the greater its value, the greater is the practical use to which it can

be put. Most of the plethora of formulae available in the literature for calculating this parameter may be mainly categorized as following from the framework of the Londons' equations or the Ginsburg-Landau (GL) equations. The salient features of such approaches are that they are based on diverse criteria such as the type of SC being dealt with (type I or II) and its geometry [1] [2] [3] [4] [5]. Another limitation of both the Londons' and the GL theories is that they work for the j_c of an SC only when its temperature T is close to its critical temperature T_c . In contrast with these *phenomenological* approaches, there is also available in the literature a smaller body of work dealing with the j_c of an SC on the basis of the *microscopic* theory of superconductivity. Notable among these is the often-used approach of Kupriyanov and Lukichev [6] based on a simplification of the Eilenberger theory, which in turn is derived from the original Gor'kov theory under the assumption that $\rho_F l \gg 1$, where ρ_F is the electrical resistivity of electrons at the Fermi surface and l their mean free path.

An overview of the study reported herein is as follows. Guided by a substantial body of recent work, e.g., [6]-[12], which suggests that *low* values of the Fermi energy (E_F) play a pivotal role in determining properties of high- T_c SCs, we have been following a course where E_F is directly incorporated into the generalized BCS equations for the gaps (Δ_s) and the T_c s of both elemental and composite SCs [13] [14]. This is a departure from the usual practice since these parameters are conventionally calculated via equations independent of E_F because of the assumption that $E_F/k\theta \gg 1$, where k is the Boltzmann constant and θ the Debye temperature of the SC. As a supplement to this framework, we reported in [15] and [16] the results of an exercise that includes an E_F -incorporated equation for j_c , leading to a unified framework for dealing with the Δ_s , T_c s and j_c s of both elemental and composite SCs at $T = 0$ and $H = 0$, where H is the applied external magnetic field. Since the j_c -values of an SC are generally reported for non-zero values of both T and H , we present here a framework to deal with such a situation. In essence, the present work is concerned with a generalization of: 1) the work reported in [17] to include E_F in the pairing equations that already incorporate T and H and 2) the work reported in [18] to include H in the equations that already incorporate T , E_F and the momentum \mathbf{P} of the pairs. We believe that presented herein is the first attempt that brings the T -and H -dependent j_c of an SC under the purview of an E_F -incorporated microscopic theory of superconductivity.

The paper is organized as follows. In Section 2, we show how, without making the usual approximation $E_F \gg k\theta$, the dynamical equation for a Cooper pair interacting via the model BCS interaction can be generalized to include T and H via the Matsubara prescription and the Landau quantization scheme, respectively. We thus obtain the pairing equation incorporating E_F , T and H corresponding to the 1-phonon exchange mechanism (1PEM) and $\mathbf{P} = 0$, which is appropriate for dealing with the situation when $j = 0$. In order to deal with the situation when $j \neq 0$, we need to do away with the $\mathbf{P} = 0$ constraint of this section.

This is done in Section 3, assuming that the dimensionless interaction parameter remains unchanged as we move out of the center-of-mass frame to the lab frame. Based on the equations thus obtained, in Section 4 are derived expressions for the density of the superconducting electrons n_s , their critical velocity v_c , j_c and $s \equiv m^*/m_e$, where m^* is the effective mass of an electron and m_e the free electron mass. Application of these equations to deal with the empirical data of $\text{Bi}_2\text{Sr}_2\text{CaCu}_2\text{O}_8$ (Bi-2212) for non-zero values of T and H is taken up in Section 5.1 (for $j = 0$) and Section 5.2 (for $j \neq 0$). In Section 5.3 we present the solutions of these equations in the scenario of 1PEM due to each of the ion species: Ca, Sr, and Bi. Sections 6 and 7 are devoted, respectively, to a Discussion of our findings and Conclusions. Finally, for the reader's convenience, we have given in an Appendix the conversion factors needed to go over from the natural system of units to the more familiar units employed in the BCS theory.

2. Pairing Equation Incorporating Fermi Energy, Temperature and Applied Field When the Momentum of Cooper Pairs Is Zero

Incorporating T and H into the pairing equation is a two-step process [17]: 1) temperature-generalization of the $T = 0$ Bethe-Salpeter Equation (BSE) via the Matsubara recipe and 2) further generalization of the equation obtained in (1) to include H via the Landau quantization scheme.

For elemental SCs for which pairing arises from the one-phonon exchange mechanism (1PEM) due to a single species of ions, Step (1) leads to

$$1 = \frac{V}{(2\pi)^3} \frac{1}{2} \int_{E_F - k\theta}^{E_F + k\theta} d^3 p \frac{\tanh\left[(\beta/2)(p^2/2m - E_F - W/2)\right]}{p^2/2m - E_F - W/2}, \quad (1)$$

where $(-V) \neq 0$ in a narrow region of $\pm k\theta$ around the Fermi surface is the model BCS interaction parameter, $\beta = 1/kT$, k is the Boltzmann constant, θ the Debye temperature of the ions, and W is one-half the binding energy of a pair which is to be identified with Δ . The units employed are: eV, $\hbar = c = 1$, generally. However, for the convenience of the reader, in all the final equations that are actually employed in our calculations, the factors of \hbar and c have been made explicit.

If the field H is applied in the z-direction, then Step (2) consists of making the following substitutions in (1):

$$\int dp_x dp_y = 2\pi eH \sum_n, \quad \frac{p_x^2}{2m} + \frac{p_y^2}{2m} = (n + 1/2)\hbar\Omega_1(H)$$

$$\Omega_1(H) = \frac{eH}{m^*c} = \Omega_0 H/s, \quad (2)$$

$$\Omega_0 = e/m_e c = 1.7588 \times 10^7 \text{ rad} \cdot \text{sec}^{-1} \cdot \text{G}^{-1}, \quad (s = m^*/m_e)$$

where $\Omega_0(H)$ is the cyclotron frequency corresponding to the free electron mass and we assume that $m^* = m_e$ when $j_c = 0$. The transverse components of momentum are thus quantized into Landau levels and we have (1) as

$$1 = \frac{eHV}{8\pi^2} \int_{-L}^L dp_z \sum_{n=0}^{n_m} \frac{\tanh\left[\frac{(\beta/2)(p_z^2/2m^* - E_F + (n+1/2)\hbar\Omega_1(H) - W/2)}{p_z^2/2m^* - E_F + (n+1/2)\hbar\Omega_1(H) - W/2}\right]}{p_z^2/2m^* - E_F + (n+1/2)\hbar\Omega_1(H) - W/2} \quad (3)$$

where L and n_m are usually ∞ . Since the energy of an electron in our problem is constrained to lie in a narrow shell around the Fermi surface, we fix L and n_m by appealing to the law of equipartition of energy and split the region in which $V \neq 0$ as

$$\begin{aligned} -\frac{2k\theta}{3} &\leq \frac{p_x^2 + p_y^2}{2m^*} = (n+1/2)\hbar\Omega_1(H) \leq \frac{2k\theta}{3} \\ -\frac{k\theta}{3} &\leq \frac{p_z^2}{2m^*} - E_F \leq \frac{k\theta}{3}. \end{aligned} \quad (4)$$

In terms of the variable $\xi = p_z^2/2m^* - E_F$, $dp_z = (1/2)\sqrt{2m^*/(E_F + \xi)}d\xi$ (3) is given by

$$\begin{aligned} 1 &= \frac{eHV}{16\pi^2} \sqrt{\frac{2m^*}{E_F}} \int_{-L_1(\theta)}^{L_1(\theta)} \frac{d\xi}{\sqrt{1 + \xi/E_F}} \\ &\times \sum_{n=0}^{n_m(\theta,H)} \frac{\tanh\left[\frac{(\beta/2)(\xi + (n+1/2)\hbar\Omega_1(H) - W/2)}{\xi + (n+1/2)\hbar\Omega_1(H) - W/2}\right]}{\xi + (n+1/2)\hbar\Omega_1(H) - W/2} \end{aligned} \quad (5)$$

where

$$L_1(\theta) = k\theta/3$$

and

$$n_m(\theta, H) = \text{floor}\left\{\frac{2k\theta}{3\hbar\Omega_1(H)} - \frac{1}{2}\right\}. \quad (6)$$

Putting $W = 0$ and rewriting (5) in terms of T and the dimensionless variable $x = \xi/\hbar\Omega_1(H_c)$, we obtain the equation for the critical field H_c at temperature T (equivalently, the equation for the critical temperature T_c at field H) as

$$\begin{aligned} 1 &= \lambda_m \int_{-L_2(\theta,H_c)}^{L_2(\theta,H_c)} \frac{dx}{\sqrt{1 + \hbar\Omega_1(H_c)x/E_{F1}}} \\ &\times \sum_{n=0}^{n_{m2}(\theta,H_c)} \frac{\tanh\left[\frac{(\hbar\Omega_1(H_c)/2kT_c)(x + n + 1/2)}{x + n + 1/2}\right]}{x + n + 1/2} \end{aligned} \quad (7)$$

where E_F has been relabeled as E_{F1} in order to distinguish it from the E_F that occurs in the equations when $\mathbf{P} \neq 0$,

$$\begin{aligned} L_2(\theta, H_c) &= k\theta/\left[3\hbar\Omega_1(H_c)\right], \\ n_{m2}(\theta, H_c) &= \text{floor}\left[2L_2(\theta, H_c) - 1/2\right] \end{aligned}$$

and

$$\lambda_m(H_c, V) = \frac{eH_c V}{16\pi^2} \sqrt{\frac{2m^*}{E_{F1}}}. \quad (8)$$

Incorporating T , H and E_{F1} (7) is the equation we had set out to obtain; it reduces to Equation (16) of [17] when $E_F \gg k\theta$. The integrand in (7) is mani-

festly dimensionless. In Appendix A, we provide the necessary conversion factors which show that λ_m too is dimensionless and enable one to employ in our framework the more familiar BCS units, *i.e.*, eV-cm³ for V and Gauss for H .

3. Pairing Equation Incorporating Fermi Energy, Temperature and Applied Field When the Momentum of Cooper Pairs Is Non-Zero

It is a tenet of the BCS theory that the same interaction parameter λ occurs in both the equation for $\{T = T_c, \Delta = 0\}$ and the equation for $\{T = 0, \Delta_0 \neq 0\}$, where Δ_0 is the gap at $T = 0$. Similarly, we assume here that λ_m remains unchanged when we go over from the $\mathbf{P} = 0$ to $\mathbf{P} \neq 0$ equations. We now draw attention to the fact that in [15] where we dealt with the Δ_0 s and j_c s of various SCs, it was assumed that E_F too has the same value in both the equation for Δ_0 ($H = 0$) and the equation for P/j_c -a plausible justification for which being that we were dealing with the j_c s too at $T = 0$ and $H = 0$. For the sake of generality, we now assume that the value of E_F when $\mathbf{P} \neq 0$ is different from its value when $\mathbf{P} = 0$. Hence, E_F is labelled as E_{F2} in the present section.

The T - and \mathbf{P} -dependent equation for pairing in the 1PEM scenario is [18]:

$$1 = \frac{V}{16\pi^2} \int_{\ell}^u d^3p \frac{\tanh[\beta C(\mathbf{p})/2] + \tanh[\beta D(\mathbf{p})/2]}{C(\mathbf{p}) + D(\mathbf{p})}, \quad (9)$$

where

$$C(\mathbf{p}) = \frac{(\mathbf{P}/2 + \mathbf{p})^2}{2m^*} - E/2 = \frac{P^2}{8m^*} + \frac{|\mathbf{P}||\mathbf{p}|\cos(\mathbf{P}, \mathbf{p})}{2m^*} + \frac{p^2}{2m^*} - E_{F2} - W/2$$

$$D(\mathbf{p}) = \frac{(\mathbf{P}/2 - \mathbf{p})^2}{2m^*} - E/2 = \frac{P^2}{8m^*} - \frac{|\mathbf{P}||\mathbf{p}|\cos(\mathbf{P}, \mathbf{p})}{2m^*} + \frac{p^2}{2m^*} - E_{F2} - W/2$$

$V \neq 0$ in the region

$$E_{F2} - k\theta \leq \frac{(\mathbf{P}/2 + \mathbf{p})^2}{2m^*}, \frac{(\mathbf{P}/2 - \mathbf{p})^2}{2m^*} \leq E_{F2} + k\theta, \quad (10)$$

and the total energy of a pair is $E = 2E_{F2} + W$. When $\mathbf{P} = 0$, (10) fixes the limits ℓ and u in (9) as $\ell = E_{F2} - k\theta$ and $u = E_{F2} + k\theta$. When $\mathbf{P} \neq 0$, the lower limit in (9) follows from:

$$E_{F2} - k\theta \leq \frac{(\mathbf{P}_c/2 - \mathbf{p})^2}{2m^*} = p^2/2m^* - |\mathbf{P}_c|p_z/2m^*, \quad (11)$$

where \mathbf{P}_c is the critical momentum corresponding to $W = 0$, $p_z = |\mathbf{p}|\cos(\mathbf{P}_c, \mathbf{p})$ and the \mathbf{P}_c^2 -term in the expansion of $(\mathbf{P}_c/2 \pm \mathbf{p})^2$ has been neglected (as justified in [18]). Note that (11) automatically ensures that $E_{F2} - k\theta < (\mathbf{P}_c/2 + \mathbf{p})^2/2m^*$. Appealing to the law of equipartition of energy as earlier, we now assume that

$$p_z^2/2m^* \cong E_{F2}/3, \text{ i.e., } p_z = \sqrt{2m^*E_{F2}/3},$$

whence we have (11) as

$$\begin{aligned}
 -E_1(\theta) + E_2(E_{F2}) &\leq \left[\left(p_z^2/2m^* - E_{F2} \right) + \left(p_x^2 + p_y^2 \right) / 2m^* \right] \\
 (E_1(\theta) = k\theta, E_2(E_{F2}) = P_c \sqrt{E_{F2}/6m^*}).
 \end{aligned}
 \tag{12}$$

which is now the lower limit in (9). Working out the upper limit similarly, we have the limits of (9) as:

$$\begin{aligned}
 -E_1(\theta) + E_2(E_{F2}) &\leq \left[\left(p_z^2/2m^* - E_{F2} \right) + \left(p_x^2 + p_y^2 \right) / 2m^* \right] \\
 &\leq E_1(\theta) - E_2(E_{F2}).
 \end{aligned}
 \tag{13}$$

Employing substitutions (2) in order to introduce H into (9), we obtain

$$\begin{aligned}
 1 &= \frac{eH_c V}{8\pi^2} \int_{-\ell_1(\theta, E_{F2})}^{\ell_1(\theta, E_{F2})} dp_z \\
 &\times \sum_{n=0}^{n_{ul}(\theta, E_{F2}, H_c)} \frac{\tanh[A_1(T_c, H_c, E_{F2}, p_z)] + \tanh[B_1(T_c, H_c, E_{F2}, p_z)]}{2 \left[\left(p_z^2/2m^* - E_{F2} \right) + (n+1/2)\hbar\Omega_2(H_c) \right]}
 \end{aligned}
 \tag{14}$$

where

$$\Omega_2(H_c) = \Omega_0 H_c / s \tag{15}$$

$$\begin{aligned}
 A_1(T_c, H_c, E_F, p_z) &= \left(\frac{1}{2kT_c} \right) \left[\left(\frac{p_z^2}{2m^*} - E_{F2} \right) + \left(n + \frac{1}{2} \right) \hbar\Omega_2(H_c) + E_2(E_{F2}) \right] \\
 B_1(T_c, H_c, E_F, p_z) &= \left(\frac{1}{2kT_c} \right) \left[\left(\frac{p_z^2}{2m^*} - E_{F2} \right) + \left(n + \frac{1}{2} \right) \hbar\Omega_2(H_c) - E_2(E_{F2}) \right]
 \end{aligned}
 \tag{16}$$

and

$$\begin{aligned}
 \ell_1(\theta, E_{F2}) &= (1/3) [E_1(\theta) - E_2(E_{F2})] \\
 n_{ul}(\theta, E_{F2}, H_c) &= \text{floor} [2\ell_1(\theta, E_{F2}) / \hbar\Omega_2(H_c) - 1/2].
 \end{aligned}$$

We note that the factors of (1/3) in the limits of the integral and (2/3) in the upper limit of the sum occur because, appealing to the equipartition law, we have split the inequalities (13) as

$$\begin{aligned}
 (1/3) [-E_1(\theta) + E_2(E_{F2})] &\leq \left(p_z^2/2m^* - E_{F2} \right) \leq (1/3) [E_1(\theta) - E_2(E_{F2})] \\
 (2/3) [-E_1(\theta) + E_2(E_{F2})] &\leq \left[\left(p_x^2 + p_y^2 \right) / 2m^* = (n+1/2)\hbar\Omega_2(H_c) \right] \\
 &\leq (2/3) [E_1(\theta) - E_2(E_{F2})].
 \end{aligned}$$

With

$$\xi = p_z^2/2m^* - E_{F2}, dp_z = \frac{1}{2} \sqrt{2m^*/(E_{F2} + \xi)} d\xi$$

(14) is transformed into

$$\begin{aligned}
 1 &= \frac{\lambda_m(V, H_c)}{2} \int_{-\ell_1(\theta, E_{F2})}^{\ell_1(\theta, E_{F2})} \frac{d\xi}{\sqrt{1 + \xi/E_{F2}}} \\
 &\times \sum_{n=0}^{n_{ul}(\theta, E_{F2}, H_c)} \frac{\tanh[A_2(T, H_c, E_{F2}, \xi)] + \tanh[B_2(T, H_c, E_{F2}, \xi)]}{\xi + (n+1/2)\hbar\Omega_2(H_c)},
 \end{aligned}
 \tag{17}$$

where $\lambda_m(V, H_c)$ is given by (8), $A_2(\dots)$ and $B_2(\dots)$ are given by $A_1(\dots)$ and $B_1(\dots)$,

respectively, with $(p_z^2/2m^* - E_{F2})$ replaced by ξ . Employing the dimensionless variables $x = \xi/\hbar\Omega_2(H_c)$ and

$$y = E_1(\theta)/E_2(E_{F2}) = \frac{k\theta}{P_c} \sqrt{6m^*/E_{F2}}, \quad (18)$$

we finally obtain the desired equation incorporating T , H and E_{F2} when $P \neq 0$ in terms of y as

$$1 = \frac{\lambda_m(V, H_c)}{2} \int_{-\ell_2(\theta, H_c, r, y)}^{\ell_2(\theta, H_c, r, y)} \frac{dx}{\sqrt{1 + \hbar\Omega_2(H_c)x/E_{F2}}} \times \sum_{n=0}^{n_{u2}(\theta, H_c, r, y)} \frac{\tanh[A_3(\dots)] + \tanh[B_3(\dots)]}{x + n + 1/2}, \quad (19)$$

where

$$\ell_2(\theta, H_c, r, y) = \frac{E_1(\theta)(1 - 1/ry)}{3\hbar\Omega_2(H_c)} \quad (20)$$

$$n_{u2}(\theta, H_c, r, y) = \text{floor}[2\ell_2(\theta, H_c, r, y) - 1/2] \quad (21)$$

$$A_3(\dots) = A_3(\theta, T_c, H_c, r, y, x, n) = \left[\frac{\hbar\Omega_2(H_c)}{2kT_c} \left\{ x + n + 1/2 + \frac{E_1(\theta)}{ry\hbar\Omega_2(H_c)} \right\} \right] \quad (22)$$

$$B_3(\dots) = B_3(\theta, T_c, H_c, r, y, x, n) = \left[\frac{\hbar\Omega_2(H_c)}{2kT_c} \left\{ x + n + 1/2 - \frac{E_1(\theta)}{ry\hbar\Omega_2(H_c)} \right\} \right]. \quad (23)$$

Although the multiplier r of y in the above equations is unity for an elemental SC, it has been introduced for later convenience when we deal with a composite SC characterized by multiple θ s. Taking the example of Bi-2212, we note that if the Debye temperature of the SC is θ_0 and pairing takes place via the Ca or the Sr ions, then $r_1 = \theta_{Ca}/\theta_0 = 1$ (because $\theta_{Ca} = \theta_0$) for the former case and $r_2 = \theta_{Sr}/\theta_0 \neq 1$ (because θ_{Sr} differs from θ_0) for the latter.

4. Equations for the Density of Superconducting Electrons, their Critical Velocity, Effective Mass, and Critical Current Density

If we assume that (7) corresponding to a set of $\{E_{F1}, T_{c1}, H_{c1}, j_{c1} = 0\}$ -values and (19) corresponding to a set of $\{E_{F2}, T_{c2}, H_{c2}, j_{c2} \neq 0\}$ -values have provided a value of y , then we are enabled to obtain the following equations for the density of superconducting electrons n_s , P_c , the critical velocity v_c and j_c , where the requisite factors of \hbar and c have been inserted for the convenience of the reader.

$$n_s(s, E_{F2}) = \frac{1}{3\pi^2} \left(\frac{2m^* E_{F2}}{(\hbar c)^2} \right)^{3/2} = C_1 (s E_{F2})^{3/2} \quad (24)$$

$$\left(C_1 = \frac{(2m_e c^2)^{3/2}}{3\pi^2 (\hbar c)^3} \cong 4.541 \times 10^{21} (\text{eV})^{-3/2} \text{ cm}^{-3} \right)$$

$$P_c(\theta, E_{F2}, s, y) = k(6sm_e)^{1/2} \frac{\theta}{y} E_{F2}^{-1/2},$$

whence

$$v_c(\theta_0, E_{F2}, s, y) = \frac{cP_c}{2sm_e} = C_2 \frac{\theta_0}{y} (sE_{F2})^{-1/2} \quad (25)$$

$$\left(C_2 = \frac{6^{1/2} ckm_e^{-1/2}}{2} \cong 4.426 \times 10^3 \text{ eV}^{1/2} \text{ K}^{-1} \text{ cm s}^{-1} \right)$$

$$j_c(\theta_0, E_{F2}, s, y) = en_s v_c = C_3 \frac{\theta_0}{y} sE_{F2} \quad (26)$$

$$\left(C_3 = eC_1 C_2 = \frac{2\sqrt{3}eckm_e}{3\pi^2 (\hbar c)^3} \cong 3.22 \times 10^6 \text{ C K}^{-1} (\text{eV})^{-1} \text{ cm}^{-2} \text{ s}^{-1} \right)$$

and

$$s(\theta, E_{F2}, j_c, r, y) = \frac{j_c r y}{C_3 \theta E_{F2}}. \quad (27)$$

5. Bi₂Sr₂CaCu₂O₈ (Bi-2212)

5.1. Pairing Equation in the 2PEM Scenario for Non-Zero Values of Temperature and Applied Field when the Critical Current Density Is Zero

We now undertake a study of Bi-2212 for which $T_c = 86$ K when $H = 0$. When $H \neq 0$, it is characterized by [19]

$$T_{c1} = 65 \text{ K}, H_{c1} = 36 \text{ Tesla}, j_{c1} = 0. \quad (28)$$

Among the 14 different values of j_c that have been reported for the same SC at different values of T and H , we focus here on the following two which are particularly interesting because they correspond to the same values of T and H :

$$T_{c2} = 4.2 \text{ K}, H_{c2} = 12 \text{ Tesla}, j_{c2} = 2.4 \times 10^5 \text{ A/cm}^2 \quad (29)$$

$$T_{c3} = T_{c2}, H_{c3} = H_{c2}, j_{c3} = 1.0 \times 10^6 \text{ A/cm}^2. \quad (30)$$

For the data in (28), we need to employ (7) which corresponds to $j_c = 0$, whereas for the data in (29) and (30) we need (19). In either case, first of all, we require the value of the Debye temperature θ_0 of the SC, which is 237 K. Since we are now dealing with a composite SC [(7) was derived for an elemental SC], we have the following multiple Debye temperatures at play because of the anisotropy of the SC [20]:

$$\theta(\text{Bi-2212}) = \theta_0 = 237 \text{ K} \quad (31)$$

$$\theta_{\text{Ca}} = 237, \theta_{\text{Sr}} = 286 \text{ K}, \theta_{\text{Bi}} = 269 \text{ K}.$$

Note that y in (18) is defined in terms of the Debye temperature of the SC (not in terms of the Debye temperature of any of the constituents of the SC if it consists of several elements). Sticking to the same definition, we have

$$y(\text{Bi-2212}) = E_1(\theta_0)/E_2(E_{F2}) = \frac{k\theta_0}{P_c} \sqrt{\frac{6sm_e}{E_{F2}}}, \quad (32)$$

and, in all the four equations following (19), we need to have [15] $r = \theta_{\text{Ca}}/\theta_0$,

$\theta_{\text{Sr}}/\theta_0$ and $\theta_{\text{Bi}}/\theta_0$ for pairing via the Ca, Sr and Bi ions, respectively.

Following our study dealing with the T_c s, Δ_0 s and j_0 s of Bi-2212 reported in [20], it seems imperative that we generalize (7) and (19) to the case of pairing via the 2PEM scenario. To this end, it is convenient to define

$$L_3(\theta, H_c) = \frac{k\theta}{3\hbar\Omega_1(H_c)}, \quad n_{u3}(\theta, H_c) = \text{floor}[2L_3(\theta, H_c) - 1/2]$$

$$\phi_1(H_c, E_F, x) = 1/\sqrt{1 + \hbar\Omega_1(H_c)x/E_F}$$

$$F_1(\theta, T_c, H_c, x) = \sum_{n=0}^{n_{u3}(\theta, H_c)} \frac{\tanh\left[\frac{\hbar\Omega_1(H_c)}{2kT_c}(x+n+1/2)\right]}{x+n+1/2}$$

$$G_1(\theta, T_c, H_c, E_{F1}) = \int_{-L_3(\theta, H_c)}^{L_3(\theta, H_c)} dx \phi_1(H_c, E_F, x) F_1(\theta, T_c, H_c, x),$$

which lead to the following equation in the 2PEM scenario as a generalization of (7) for pairing via the Ca and Sr ions when $j_c = 0$:

$$\begin{aligned} & Eq1(\theta_1, \theta_2, T_{c1}, H_{c1}, E_{F1}, \lambda_{m1}, \lambda_{m2}) \\ & \equiv \text{Re}\left[1 - \lambda_{m1}G_1(\theta_1, T_{c1}, H_{c1}, E_{F1}) - \lambda_{m2}G_1(\theta_2, T_{c1}, H_{c1}, E_{F1})\right] = 0. \end{aligned} \quad (33)$$

For the θ -values in (31), we note that (i) solution of (33) with inputs from (28) leads to (a) the value of λ_{m1} for pairing in the 1PEM scenario via the Ca ions by putting $\theta_1 = \theta_{\text{Ca}}$, $\lambda_{m2} = 0$ and (b) the value of λ_{m2} for pairing in the 1PEM scenario via the Sr ions by putting $\lambda_{m1} = 0$, $\theta_2 = \theta_{\text{Sr}}$ and (ii) the need to invoke 2PEM will arise only if either of the so-obtained λ_{m} s exceeds the Bogoliubov limit of 0.5, because beyond this value the system becomes unstable.

5.2. Pairing Equation in the 2PEM Scenario for Non-Zero Values of Temperature, Applied Field and Critical Current Density

If we obtain the generalized version of (19) to deal with pairing in the 2PEM scenario following the same procedure as above, then with the inputs from (29) and (30) we have two equations besides (33). These three equations are not sufficient to deal with at least the six unknowns in our problem: λ_{m1} , λ_{m2} , E_{F1} , E_{F2} , E_{F3} and y . Therefore, ab-initio calculation of the j_c s via this approach will involve making ad hoc assumptions about some of the unknowns. To avoid such a situation, we adopt the strategy of incorporating in the generalized version of (19) the empirical j_c -values noted in (29) or (30). Even though the number of equations in this approach continues to be three, we show below how it sheds light on several important features of the data in (29) and (30).

In order to incorporate j_c into (19), we employ (27) for $s(\theta, E_F, j_c, r, y)$, whence we have (15) as

$$\Omega_2(H_c) \rightarrow \Omega_2(\theta, H_c, E_F, j_c, r, y) = \frac{C_3\Omega_0 H_c \theta E_F}{j_c r y}$$

and (20)-(23) as

$$\ell_4(H_c, E_F, j_c, r, y) = \frac{k j_c (ry - 1)}{3C_3 \hbar \Omega_0 H_c E_F} \quad (34)$$

$$n_{u4}(H_c, E_F, j_c, r, y) = \text{floor} \left[2\ell_4(H_c, E_F, j_c, r, y) - 1/2 \right] \quad (35)$$

$$\begin{aligned} A_3(\dots) &= A_3(\theta, T_c, H_c, E_F, j_c, r, y, x, n) \\ &= \left[\frac{\hbar \Omega_2(\theta, H_c, E_F, j_c, r, y)}{2kT_c} \left\{ x + n + \frac{1}{2} + \frac{k\theta}{\hbar \Omega_2(\theta, H_c, E_F, j_c, r, y)} \right\} \right] \end{aligned} \quad (36)$$

$$\begin{aligned} B_3(\dots) &= B_3(\theta, T_c, H_c, E_F, j_c, r, y, x, n) \\ &= \left[\frac{\hbar \Omega_2(\theta, H_c, E_F, j_c, r, y)}{2kT_c} \left\{ x + n + 1/2 - \frac{k\theta}{\hbar \Omega_2(\theta, H_c, E_F, j_c, r, y)} \right\} \right]. \end{aligned} \quad (37)$$

With the definitions

$$\phi_2(\theta, H_c, E_F, j_c, x, r, y) = \frac{1}{\sqrt{1 + \hbar \Omega_2(\theta, H_c, E_F, j_c, r, y) x / E_F}}$$

$$F_2(\theta, T_c, H_c, E_F, j_c, x, r, y) = \sum_{n=0}^{n_{u4}(H_c, E_F, j_c, r, y)} \frac{A_3(\dots) + B_3(\dots)}{x + n + 1/2},$$

where $\ell_4(\dots)$, $n_{u4}(\dots)$, $A_3(\dots)$ and $B_3(\dots)$ are given by (34), (35), (36) and (37), respectively, and

$$G_2(\theta, T_c, H_c, E_F, j_c, r, y) = \int_{-\ell_4(\dots)}^{\ell_4(\dots)} dx \phi_2(\dots) F_2(\dots), \quad (38)$$

we obtain, in the 2PEM scenario as a generalization of (19) for pairing via two species of ions and a given value of j_c , the following equation:

$$\begin{aligned} &Eq2(\theta_1, \theta_2, T_c, H_c, q, E_F, j_c, r_1, r_2, y, \lambda_{m1}, \lambda_{m2}) \\ &\equiv \text{Re} \left[1 - \lambda_{m1} G_2(\theta_1, T_c, H_c, E_F, j_c, r_1, y) - \lambda_{m2} G_2(\theta_2, T_c, H_c, E_F, j_c, r_2, y) \right] = 0. \end{aligned} \quad (39)$$

5.3. Solutions in the Scenario of 1PEM Due to Either of the Ca, Bi and the Sr Ions

In order to unravel the empirical features of Bi-2212 noted in (28), (29) and (30) in the above framework, we proceed as follows:

1) We first deal with the data in (28) via (33) where, in the latter equation, E_{F1} is an independent variable. If we solve this equation for different assumed values of $E_{F1} = \rho k \theta_0$ and $\lambda_{m2} = 0$, we obtain the corresponding values of λ_{m1} for pairing via the Ca ions. We thus find that for $\rho = 10$, $\lambda_{m1} = 0.31283$ and for all values of $\rho > 10$, λ_{m1} has the same value up to four significant digits. For the same value of ρ and $\lambda_{m1} = 0$, the corresponding value of $\lambda_{m2}(\text{Bi})$ and $\lambda_{m2}(\text{Sr})$ via (33) are 0.22043 and 0.20778, respectively. Similarly obtained values of $\lambda_{m1}(\text{Ca})$, $\lambda_{m2}(\text{Bi})$ and $\lambda_{m2}(\text{Sr})$ for some select values of $\rho \leq 10$ are given in **Table 1**.

2) Since none of the values of λ_m in **Table 1** exceeds the Bogoliubov limit of 0.5, we now employ (39) also in the 1PEM scenario in order to determine E_{F2} corresponding to the data in (29). To this end for $\rho = 10$, for pairing via the Ca ions, we use the following values in (39):

Table 1. Obtained via (33), the interaction parameters $\lambda_{m1}(\text{Ca})$, $\lambda_{m2}(\text{Bi})$ and $\lambda_{m2}(\text{Sr})$ for pairing via the Ca, Bi, and Sr ions corresponding to $T_{c1} = 65 \text{ K}$, $H_{c1} = 36 \times 10^4 \text{ G}$ with the additional inputs $\{\lambda_{m2} = 0, \theta_1 = 237\}$, $\{\lambda_{m1} = 0, \theta_2 = 269 \text{ K}\}$ and $\{\lambda_{m1} = 0, \theta_2 = 286 \text{ K}\}$, respectively.

$\rho = \frac{E_{F1}}{k\theta_0}$	$\lambda_{m1}(\text{Ca})$	$\lambda_{m2}(\text{Bi})$	$\lambda_{m2}(\text{Sr})$
10	0.31283	0.22043	0.20778
5	0.31243	0.22003	0.20736
4	0.31219	0.21980	0.20712
3	0.31176	0.21937	0.20667
2	0.31069	0.21835	0.20558
1	0.30594	0.21382	0.20075

$$\begin{aligned} \lambda_{m2} = 0, \lambda_{m1} = 0.31283; T_c = T_{c2}, H_c = H_{c2}, j_c = j_{c2}; \\ r = r_1 = 1, E_F = qE_{F1} \quad (E_{F1} = \rho k\theta_0), \end{aligned} \quad (40)$$

which leaves out y which is yet to be specified. Since y too is an independent variable, we need to solve (39) for a range of values of $ry > 1$; that ry must be greater than unity follows from (34). We find that for each such value of y , the solution of the transcendental Equation (39) yields, in general, multiple roots *each* of which corresponds not only to j_{c2} (which is an in-built feature of our formalism), but also, to the accuracy with which they are quoted in **Table 2** and **Table 3**, the same values for n_s and v_c via (24) and (25), respectively. For this reason, corresponding to each y , given in **Table 2** are only the greatest roots of (39), which are found by first plotting (39) against q to determine the range outside which the equation does not have any roots.

In the context of the critical current densities, such a plot given in **Figure 1** seems to be unusual and will be discussed below. The largest value of q corresponding to any value of y at which the function being plotted crosses zero is then found more accurately using numerical root-finding methods and is given in **Table 2** where similar results for $\rho = 5$ and 1 for both pairings via the Ca and the Sr ions are also given.

The parameters, the values of which are different for different roots, corresponding to the same value of y are n_{i4} , s and E_{F2} where n_{i4} and s are determined via (35) and (27), respectively, and $E_{F2} = qE_{F1}$. Of these, the values of s dictate the range of y relevant for the data under consideration. To elaborate, for $y \leq 2.40$, it is found that $s \geq 37$. Since, contrary to the known features of the SC under consideration, such values of s would put it in the category of heavy-fermion SCs [13], they must be excluded and so we set the lower limit of y at a value which leads to $s \approx 10$. The value of s decreases as y is progressively increased. This feature enables us to set the upper limit on the value of y as one for which $s \approx 1$.

3) For the data in (30), we also give in **Table 3** the results that follow when the operative IPEM is due to the Sr ions.

Table 2. The largest values of $q \equiv E_{F2}/E_{F1}$ corresponding to y_1 and y_2 obtained by solving (39) for the set $S_1 = \{T_c, H_c, j_c, \text{ion species}\}$ as noted and different pairs of $S_2 = \{\rho, \lambda_m\}$ values taken from **Table 1**. n_{u1}, s, n_s and v_c corresponding to q_1 and q_2 are calculated via (35), (27), (24) and (25), respectively.

$T_c = T_{c2} = 4.2 \text{ K}, H_c = H_{c2} = 12 \times 10^4 \text{ G}, j_c = j_{c2} = 2.4 \times 10^5 \text{ A} \cdot \text{cm}^{-2}$, Pairing via Ca ions							
ρ, λ	y_1, y_2 as in $y_1 \leq y \leq y_2$	q_1, q_2 as in $q_1 \leq q \leq q_2$ ($\times 10^{-4}$)	n_{u1}, n_{u2} as in $n_1 \geq n_{u4} \geq n_2$	s_1, s_2 as in $s_1 \geq s \geq s_2$	n_{s1}, n_{s2} as in $n_{s1} \leq n_s \leq n_{s2}$ ($\times 10^{17} \text{ cm}^{-3}$)	v_{c1}, v_{c2} as in $v_{c1} \geq v_c \geq v_{c2}$ ($\times 10^7 \text{ cm/s}$)	$E_{F2}^1 = q_1 E_{F1}$ $E_{F2}^2 = q_2 E_{F1}$ $E_{F2}^1 \leq E_{F2} \leq E_{F2}^2$ ($\times 10^{-4} \text{ eV}$)
10, 0.31283	2.575, 3.10	4.5194, 48.041	52, 6	8.77, 0.99	1.05, 1.38	1.43, 1.08	0.92, 9.81
5, 0.31243	2.575, 3.10	9.0422, 96.168	52, 6	8.77, 0.99	1.05, 1.38	1.43, 1.08	0.92, 9.82
1, 0.30594	2.575, 3.20	43.589, 472.32	54, 6	9.10, 1.04	1.05, 1.45	1.43, 1.03	0.89, 9.65
$T_c = T_{c2} = 4.2 \text{ K}, H_c = H_{c2} = 12 \times 10^4 \text{ G}, j_c = j_{c2} = 2.4 \times 10^5 \text{ A} \cdot \text{cm}^{-2}$, Pairing via Sr ions							
10, 0.20778	2.50, 3.35	3.9111, 49.813	77, 8	9.84, 1.04	1.00, 1.55	1.50, 0.96	0.80, 10.2
5, 0.2076	2.50, 3.35	7.9476, 99.83	76, 8	9.69, 1.03	1.00, 1.55	1.50, 0.96	0.81, 10.2
1, 0.20075	2.51, 3.35	39.478, 516.30	77, 8	9.79, 1.00	1.01, 1.55	1.49, 0.96	0.81, 10.5

Table 3. The largest values of $q \equiv E_{F2}/E_{F1}$ corresponding to y_1 and y_2 obtained by solving (39) for the set $S_1 = \{T_c, H_c, j_c, \text{ion species}\}$ as noted and different pairs of $S_2 = \{\rho, \lambda_m\}$ values taken from **Table 1**. n_{u1}, s, n_s and v_c corresponding to q_1 and q_2 are calculated via (35), (27), (24) and (25), respectively.

$T_c = T_{c3} = 4.2 \text{ K}, H_c = H_{c3} = 12 \times 10^4 \text{ G}, j_c = j_{c3} = 1.0 \times 10^6 \text{ A} \cdot \text{cm}^{-2}$, Pairing via Ca ions							
ρ, λ	y_1, y_2 as in $y_1 \leq y \leq y_2$	q_1, q_2 as in $q_1 \leq q \leq q_2$ ($\times 10^{-3}$)	n_{u1}, n_{u2} as in $n_1 \geq n_{u4} \geq n_2$	s_1, s_2 as in $s_1 \geq s \geq s_2$	n_{s1}, n_{s2} as in $n_{s1} \leq n_s \leq n_{s2}$ ($\times 10^{17} \text{ cm}^{-3}$)	v_{c1}, v_{c2} as in $v_{c1} \geq v_c \geq v_{c2}$ ($\times 10^6 \text{ cm/s}$)	$E_{F2}^1 = q_1 E_{F1}$ $E_{F2}^2 = q_2 E_{F1}$ $E_{F2}^1 \leq E_{F2} \leq E_{F2}^2$ ($\times 10^{-4} \text{ eV}$)
10, 0.31283	2.40, 2.90	1.5499, 17.720	56, 6	9.94, 1.05	8.01, 10.6	7.79, 5.87	3.17, 36.2
5, 0.31243	2.40, 2.90	3.2281, 35.461	54, 6	9.54, 1.05	8.01, 10.6	7.79, 5.87	3.30, 36.2
1, 0.30594	2.40, 2.90	15.274, 179.10	57, 6	10.08, 1.04	8.01, 10.6	7.79, 5.87	3.12, 36.6
$T_c = T_{c3} = 4.2 \text{ K}, H_c = H_{c3} = 12 \times 10^4 \text{ G}, j_c = j_{c3} = 1.0 \times 10^6 \text{ A} \cdot \text{cm}^{-2}$, Pairing via Sr ions							
10, 0.20778	2.30, 2.90	1.4543, 20.791	76, 7	10.15, 0.89	7.51, 10.6	8.31, 5.87	2.97, 42.5
5, 0.20736	2.30, 2.90	2.9099, 35.048	76, 8	10.14, 1.06	7.51, 10.6	8.31, 5.87	2.97, 35.8
1, 0.20075	2.31, 2.90	14.619, 177.80	76, 8	10.14, 1.05	7.56, 10.6	8.25, 5.87	2.99, 36.3

4) Pairing in Bi-2212 can of course also take place via the Bi ions in the 1PEM scenario. From the results obtained via the Ca and the Sr ions and the value of θ_{Bi} , which lies between θ_{Ca} and θ_{Sr} [vide (31)], one would expect that $\lambda_m(\text{Bi})$ for any of the value of ρ in either of the two Tables should lie between the corresponding values of $\lambda_m(\text{Ca})$ and $\lambda_m(\text{Sr})$ and that, but for this change, the overall results should be substantially similar to those already obtained. This is indeed found to be so, as can be seen from the following results corresponding to $T = 4.2 \text{ K}$, $H_c = 12 \times 10^4 \text{ G}$ and $j_c = 2.4 \times 10^5 \text{ A/cm}^2$ as an example:

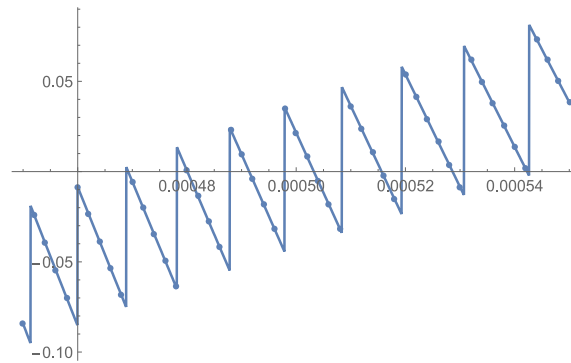


Figure 1. Plot of Eq 2 ($\theta_1, \theta_2, T_{c2}, H_{c2}, q, E_{F1}, j_{c2}, n_1, n_2, y, \lambda_{m1}, 0$)vide (39) as a function of q showing multiple roots of (39) in the indicated range corresponding to $\theta_1 = 237, n_1 = 1, \rho = 10, \lambda_{m1} = 0.31283, y = 2.60$ and $\{T_{c2}, H_{c2}, j_{c2}\}$ as in (29).

$$\begin{aligned} \rho &= 10, \lambda = 0.22043; 2.54 \leq y \leq 3.30 \\ 4.0226 \times 10^{-4} &\leq q \leq 5.4521 \times 10^{-3}, 70 \geq n_u \geq 7, 9.72 \geq s \geq 0.93 \\ 1.03 \times 10^{17} &\leq n_s \leq 1.52 \times 10^{17}, 1.46 \times 10^7 \geq v_c \geq 9.87 \times 10^6 \\ 0.82 \times 10^{-4} &\leq E_{F2} \leq 11.1 \times 10^{-4}, \end{aligned}$$

where the units for n_s, v_c and E_F are $\text{cm}^{-3}, \text{cm/s}$ and eV , respectively.

6. Discussion

To give a perspective of the approach followed in this paper, it is pertinent to point out that, conventionally, the j_c of an SC is determined via one or the other critical state models; for characteristic equations of *nine* critical state models, see ([19], p61). It is postulated in such models that for low applied fields or currents the outer part of the sample is in the so-called critical state which is characterized by particular values of j_c and H and that the interior of the SC is shielded from these fields and currents. For Bi-2212, the most commonly employed model is Bean's model where its j_c is determined via the geometry of the sample and the magnetization width ΔM of the $M(H)$ hysteresis loop; see, e.g. [21], which gives values of $j_c(H)$ of the melt quenched and the non-melted samples of the SC at 5 K. Following the conventional approach, the significantly different $j_c(H)$ -values of the samples in [21] are attributed to material properties of the samples such as their cell parameters, alignment and inter-connectivity of the grains and the grain boundaries. It is hence seen that the approach followed in our paper differs radically from the conventional approach.

A remark about the operator Re in (33): The function $G_1(\theta_1, T_{c1}, H_{c1}, E_{F1})$ in this equation becomes pure imaginary for all values of $x < -E_F/\hbar\Omega_1(H_c)$ because of $\phi_1(H_{c1}, E_{F1}, x)$. This is a situation which also occurs in several other problems, e.g., while dealing with heavy-fermion SCs [13] and BCS-BEC crossover [22]. In order then to obtain real solutions, one alternative is to manually shift the lower limit of integration. This becomes cumbersome if one is simultaneously dealing with more than one such equation. The operator Re provides a much simpler, one-step, alternative, as was also noted in the context of Fe-based

SCs [23]. This remark also applies to (39).

As was noted above, the solution of (39) leads to multiple roots for any value of γ for which s falls in the range of our interest. These are shown in **Figure 1** for a particular value of γ . A notable feature of this figure is its saw-tooth appearance (a series of “Vs”), which is attributable to a *combination* of the fluctuations in Fermi energy and the floor function employed in our formalism. The unmarked vertical limbs of the Vs are discontinuities which occur when the summation index n changes discretely from one integral value to another due to the floor function. We note that no root is found even when such limbs cross zero, as also that the saw-tooth behavior is not seen when (33) is solved despite the fact that it too employs the floor function, which is so because it is solved for a *fixed* value of E_F .

Another feature of (39) is that as γ is progressively increased, the number of its roots keeps decreasing, as an example of which we note that as one goes from $\gamma = 2.60$ to 3.10 in the upper-half of **Table 2**, the number of roots changes from 7 to 2. This is reminiscent of Melde’s experiment with stationary waves on a taut string clamped at both ends which are therefore nodal points. In-between these, the string displays a varying number of nodes depending on the frequency of the tuning fork with which it is induced to vibrate. One is thus led to surmise that: 1) (39) embodies content that leads to behavior akin to a Melde’s string, 2) the variation of γ in the present case is equivalent to changing the frequency of the tuning fork and 3) the values of q at which (39) vanishes (*i.e.*, the roots of the equation) are equivalent to the nodes of the Melde’s string.

Regarding the employment of Ω_0 (which corresponds to free electron mass) in obtaining solutions of (33), we note that there is no loss of generality in making this assumption in so far as the solutions of this equation are employed to shed light on why the same SC at the same values of T and H sustains different values of j_c —which is the chief objective of this study. This assertion follows from the fact that different pairs of $\{\rho, \lambda_m\}$ in both **Table 2** and **Table 3** lead to essentially similar results for each of the following parameters: n_{u4}, s, n_s, v_c and E_F .

In so far as the n_u values given in **Table 2** and **Table 3** are concerned, we recall from [17] that the radius of the largest Landau orbit is given by

$$r_n(H) = r_0 \sqrt{2n_u(H) + 1}$$

where $r_0 = \sqrt{\hbar c / e H_0}$ and H_0 is the critical applied field at $T = 0$ and that $n_u(H_0)$ for the elemental SCs Hg, In, Tl and Sn, for example, has the values 1062, 1900, 2201 and 3172, respectively. Since $r_n(H)$ and therefore n_u may also be regarded as a measure of the coherence length of the SC, the low values of the latter in the two Tables signify that Bi-2212 has a much smaller coherence length than the elemental SCs, which is in accord with the known empirical facts.

If, for both the values of j_c , *i.e.*, $j_{c2} = 2.4 \times 10^5$ (for an Ag-sheathed tape) and $j_{c3} = 1.0 \times 10^6$ A/cm² (for a multilayer tape), the SC is assumed to have nearly the same value of s , which is unlikely, then the results in **Table 2** and **Table 3** show that 1) $n_s(j_{c2}) < n_s(j_{c3})$, 2) $v_c(j_{c2}) > v_c(j_{c3})$ and 3) $E_F(j_{c2}) < E_F(j_{c3})$. All

of these results remain valid even if $s(j_{c2}) \approx 10$ and $s(j_{c3}) \approx 1$. However, if $s(j_{c2}) \approx 1$ and $s(j_{c3}) \approx 10$ then, while the first two results still hold, we have $E_F(j_{c2}) > E_F(j_{c3})$. In so far as the absolute values of E_F in **Table 2** and **Table 3** are concerned, the lowest among them are of the order of 0.3 meV or less; these are interpretable as being near the nodes or the node lines on the Fermi surface.

7. Conclusions

1) Based on the microscopic BSE customized to deal with superconductivity, we have given here derivation of equations that incorporate E_F (equivalently, the chemical potential μ), T , H , and P .

2) Among the main results of this paper are (33) and (39). The former generalizes the equation given in [17] that incorporated T and H , but not E_F ; the latter generalizes the equation given in [18] that incorporated T , E_F and P , but not H .

3) Another notable result of the approach followed here is that it sheds light on why the cuprate that we have dealt with has much smaller coherence length than elemental SCs.

4) A novel aspect of our work is that it incorporates j_c , which is a sample-specific property, into the dynamical equations that govern pairing in the SC.

5) As is well-known, the j_c of an SC depends on several factors such as its size, shape, and how it is doped and prepared. Based on the premise that the E_F of an SC subsumes all of these features, we have given here a framework for testing it, and applied it for a detailed study of Bi-2212.

6) The upshot of the present work is that for greater substantiation of the above premise, there is a need not only to monitor via experiment, insofar as it may be feasible, the following parameters for Bi-2212: n_{u4} , s , n_s and v_c , but also to carry out similar studies for other SCs. Unfortunately, none of the conventionally employed critical state models sheds light on any of these parameters.

We conclude by noting that a detailed exposition of most of concepts of the BSE-based approach employed in this paper can be found in [24].

Acknowledgements

GPM thanks Dr. V.P.S. Awana for a valuable discussion of the conventional critical state models and the approach followed in this paper for determining the j_c of an SC. It is gratifying to note that invoking the electronic structure of an SC in this context, as done here, seemed to be a refreshing new approach to him.

Conflicts of Interest

The authors declare no conflicts of interest regarding the publication of this paper.

References

- [1] Tinkham, M. (1975) Introduction to Superconductivity. McGraw Hill, New York.

- [2] Ibach, H. and Lüth, H. (1996) Solid State Physics. Springer, Berlin. <https://doi.org/10.1007/978-3-642-88199-2>
- [3] Bardeen, J. (1962) Critical Fields and Currents in Superconductors. *Reviews of Modern Physics*, **34**, 667-681. <https://doi.org/10.1103/RevModPhys.34.667>
- [4] Bean, C.P. (1964) Magnetization of High-Field Superconductors. *Reviews of Modern Physics*, **36**, 31-39. <https://doi.org/10.1103/RevModPhys.36.31>
- [5] Kim, Y.B., Hempstead, C.F. and Strand, A.R. (1963) Magnetization and Critical Supercurrents. *Physical Review*, **129**, 528-535. <https://doi.org/10.1103/PhysRev.129.528>
- [6] Kupriyanov, M.Y. and Lukichev, V.F. (1980) Temperature Dependence of Pair-Breaking Current in Superconductors. *Soviet Journal of Low Temperature Physics*, **6**, 210.
- [7] Lee, D. (2012) Iron-Based Superconductors: Nodal Rings. *Nature Physics*, **8**, 364-365. <https://doi.org/10.1038/nphys2301>
- [8] Zhang, Y., *et al.* (2012) Nodal Superconducting Gap-Structure in Ferropnictide Superconductor $\text{Ba}_2\text{Fe}_2(\text{As}_{0.7}\text{P}_{0.3})_2$. *Nature Physics*, **8**, 371-375. <https://doi.org/10.1038/nphys2248>
- [9] Allan, M.P., *et al.* (2012) Anisotropic Energy Gaps of Iron-Based Superconductivity from Intraband Quasiparticle Interference in LiFeAs. *Science*, **336**, 563-567. <https://doi.org/10.1126/science.1218726>
- [10] Lin, X., *et al.* (2013) Fermi Surface of the Most Dilute Superconductor. *Physical Review X*, **3**, Article ID: 021002. <https://doi.org/10.1103/PhysRevX.3.021002>
- [11] Alexandrov, A.S. (2001) Nonadiabatic Polaronic Superconductivity in MgB_2 and Cuprates. *Physica C: Superconductivity*, **363**, 231-236. [https://doi.org/10.1016/S0921-4534\(01\)01095-4](https://doi.org/10.1016/S0921-4534(01)01095-4)
- [12] Jarlborg, T. and Bianconi, A. (2013) Fermi Surface Reconstruction of Superoxygenated La_2CuO_4 Superconductors with Ordered Oxygen Interstitials. *Physical Review B*, **87**, Article ID: 054514. <https://doi.org/10.1103/PhysRevB.87.054514>
- [13] Malik, G.P. (2015) A Study of Heavy-Fermion Superconductors via BCS Equations Incorporating Chemical Potential. *Journal of Modern Physics*, **6**, 1233-1242. <https://doi.org/10.4236/jmp.2015.69128>
- [14] Malik, G.P. and Varma, V.S. (2015) A Study of Superconducting La_2CuO_4 via Generalized BCS Equations Incorporating Chemical Potential. *World Journal of Condensed Matter Physics*, **5**, 148-159. <https://doi.org/10.4236/wjcmp.2015.53017>
- [15] Malik, G.P. (2016) On the Role of Fermi Energy in Determining Properties of Superconductors: A Detailed Comparative Study of Two Elemental Superconductors (Sn and Pb), a Non-Cuprate (MgB_2) and Three Cuprates (YBCO, Bi-2212 and Tl-2212). *Journal of Superconductivity and Novel Magnetism*, **29**, 2755-2764. <https://doi.org/10.1007/s10948-016-3637-5>
- [16] Malik, G.P. (2018) Correction to: On the Role of Fermi Energy in Determining Properties of Superconductors: A Detailed Comparative Study of Two Elemental Superconductors (Sn and Pb), a Non-Cuprate (MgB_2) and Three Cuprates (YBCO, Bi-2212 and Tl-2212). *Journal of Superconductivity and Novel Magnetism*, **31**, 941-941. <https://doi.org/10.1007/s10948-017-4520-8>
- [17] Malik, G.P. (2010) On Landau Quantization of Cooper Pairs in a Heat Bath. *Physica B*, **405**, 3475-3481. <https://doi.org/10.1016/j.physb.2010.05.026>
- [18] Malik, G.P. (2013) On a New Equation for Critical Current Density in Terms of the BCS Interaction Parameter, Debye Temperature and the Fermi Energy of the Su-

perconductor. *World Journal of Condensed Matter Physics*, **3**, 103-110.

<https://doi.org/10.4236/wjcmp.2013.32017>

- [19] Poole, C.P. (2000) Handbook of Superconductivity. Academic Press, San Diego.
- [20] Malik, G.P. and Varma, V.S. (2019) Generalized BCS Equations: A Review and a Detailed Study of the Superconducting Features of $\text{Ba}_2\text{Sr}_2\text{CaCu}_2\text{O}_8$. In: *Superconductivity and Superfluidity*, IntechOpen, London, 21 p.
<https://doi.org/10.5772/intechopen.84340>
- [21] Kumar, J., Sharma, D., Ahluwalia, P.K. and Awana, V.P.S. (2013) Enhanced Superconducting Performance of Melt Quenched $\text{Bi}_2\text{Sr}_2\text{CaCu}_2\text{O}_8$ (Bi-2212) Superconductor. *Materials Chemistry and Physics*, **139**, 681-688.
<https://doi.org/10.1016/j.matchemphys.2013.02.016>
- [22] Malik, G.P. (2014) BCS-BEC Crossover without Appeal to Scattering Length Theory. *International Journal of Modern Physics B*, **8**, Article ID: 1450054.
<https://doi.org/10.1142/S0217979214500544>
- [23] Malik, G.P. (2017) On the S^\pm -Wave Superconductivity in the Iron-Based Superconductors: A Perspective Based on a Detailed Study of $\text{Ba}_{0.6}\text{K}_{0.4}\text{Fe}_2\text{As}_2$ via the Generalized Bardeen-Cooper-Schrieffer Equations Incorporating Fermi Energy. *Open Journal of Composite Materials*, **7**, 130-145.
<https://doi.org/10.4236/ojcm.2017.73008>
- [24] Malik, G.P. (2016) Superconductivity: A New Approach Based on the Bethe-Salpeter Equation in the Mean-Field Approximation. Volume 21 in the Series on Directions in Condensed Matter Physics. World Scientific, Singapore.
<https://doi.org/10.1142/9868>

Appendix A

In order to see that λ_m defined in (8) in the natural system of units is dimensionless, we need the following conversion factors:

$$1 \text{ g} = a_1 e V c^{-2}, \quad 1 \text{ cm} = a_2 e V^{-1} (\hbar c), \quad e = b_1 (\hbar c)^{1/2},$$

$$1 \text{ s} = a_3 e V^{-1} \hbar, \quad 1 \text{ G} = \text{g}^{1/2} \cdot \text{cm}^{-1/2} \cdot \text{s}^{-1} = b_2 e V^2 (\hbar c)^{-3/2},$$

where

$$a_1 = 5.60958616 \times 10^{32}, \quad a_2 = 5.06772886 \times 10^4, \quad a_3 = 1.51926689 \times 10^{15}$$

$$b_1 = (137.03599895)^{-1/2}, \quad b_2 = a_1^{1/2} a_2^{-1/2} a_3^{-1} = 6.92507774 \times 10^{-2}.$$

Hence, we have

$$e = b_1 (\hbar c)^{1/2} = b_1 \quad (\text{if } \hbar = c = 1) \quad (\text{A1})$$

$$H_c(BCS, G) = b_2 |H_c| e V^2 (\hbar c)^{-3/2} = b_2 |H_c| e V^2 \quad (\text{if } \hbar = c = 1) \quad (\text{A2})$$

$$V_{BCS} = |V| e V c m^3 = a_2^3 |V| e V^{-2} (\hbar c)^3 = a_2^3 |V| e V^{-2} \quad (\text{if } \hbar = c = 1) \quad (\text{A3})$$

It follows from the above equations that when $\hbar \neq 1$ and $c \neq 1$, V_{BCS} has to be divided by $(\hbar c)^3$ in order for it to play the required role of a propagator in the BSE-based approach and that, after inserting a factor of $\hbar c$ on the RHS of the first equation in the set of Equations (2), we obtain

$$\lambda_m = \frac{a_2^3 b_1 b_2 |H| |V|}{16\pi^2} \sqrt{\frac{2m^* c^2}{E_F}}, \quad (\text{A4})$$

which is dimensionless, since both $|H|$ and $|V|$ are pure numbers.

We note that (A4) is needed only when one wishes to decouple the constituent V of λ_m after the latter has been determined corresponding to a given value of H .